

# The Silicon Vertex Detector of the Belle II experiment

A.B. Kaliyar<sup>a,\*</sup> K. Adamczyk<sup>b</sup> L. Aggarwal<sup>c</sup> H. Aihara<sup>d</sup> T. Aziz<sup>e</sup> S. Bacher<sup>b</sup>  
 S. Bahinipati<sup>f</sup> G. Batignani<sup>g,h</sup> J. Baudot<sup>i</sup> P. K. Behera<sup>j</sup> S. Bettarini<sup>g,h</sup> T. Bilka<sup>k</sup>  
 A. Bozek<sup>b</sup> F. Buchsteiner<sup>a</sup> G. Casarosa<sup>g,h</sup> L. Corona<sup>h</sup> S. B. Das<sup>l</sup> G. Dujany<sup>i</sup>  
 C. Finck<sup>i</sup> F. Forti<sup>g,h</sup> M. Friedl<sup>a</sup> A. Gabrielli<sup>m,n</sup> B. Gobbo<sup>n</sup> S. Halder<sup>e</sup> K. Hara<sup>o,p</sup>  
 S. Hazra<sup>e</sup> T. Higuchi<sup>q</sup> C. Irmler<sup>a</sup> A. Ishikawa<sup>o,p</sup> Y. Jin<sup>n</sup> M. Kaleta<sup>b</sup> J. Kandra<sup>k</sup>  
 K. H. Kang<sup>q</sup> P. Kodyš<sup>k</sup> T. Kohriki<sup>o</sup> R. Kumar<sup>r</sup> K. Lalwani<sup>l</sup> K. Lautenbach<sup>t</sup>  
 R. Leboucher<sup>t</sup> S. C. Lee<sup>s</sup> J. Libby<sup>j</sup> L. Martel<sup>i</sup> L. Massaccesi<sup>g,h</sup> G. B. Mohanty<sup>e</sup>  
 S. Mondal<sup>g,h</sup> K. R. Nakamura<sup>o,p</sup> Z. Natkaniec<sup>b</sup> Y. Onuki<sup>d</sup> F. Otani<sup>q</sup>  
 A. Paladino<sup>A, g,h</sup> E. Paoloni<sup>g,h</sup> H. Park<sup>s</sup> L. Polat<sup>t</sup> K. K. Rao<sup>e</sup> I. Ripp-Baudot<sup>i</sup>  
 G. Rizzo<sup>g,h</sup> Y. Sato<sup>o</sup> C. Schwanda<sup>a</sup> J. Serrano<sup>t</sup> T. Shimasaki<sup>q</sup> J. Suzuki<sup>o</sup>  
 S. Tanaka<sup>o,p</sup> H. Tanigawa<sup>d</sup> F. Tenchini<sup>g,h</sup> R. Thalmeier<sup>a</sup> R. Tiwary<sup>e</sup>  
 T. Tsuboyama<sup>o</sup> Y. Uematsu<sup>d</sup> L. Vitale<sup>m,n</sup> Z. Wang<sup>d</sup> J. Webb<sup>u</sup> O. Werbycka<sup>n</sup>  
 J. Wiechczynski<sup>b</sup> H. Yin<sup>a</sup> and L. Zani<sup>B,t</sup>

<sup>a</sup>Institute of High Energy Physics, Austrian Academy of Sciences, 1050 Vienna, Austria

<sup>b</sup>H. Niewodniczanski Institute of Nuclear Physics, Krakow 31-342, Poland

<sup>c</sup>Punjab University, Chandigarh 160014, India

<sup>d</sup>Department of Physics, University of Tokyo, Tokyo 113-0033, Japan

<sup>e</sup>Tata Institute of Fundamental Research, Mumbai 400005, India

<sup>f</sup>Indian Institute of Technology Bhubaneswar, Bhubaneswar 752050, India

<sup>g</sup>Dipartimento di Fisica, Università di Pisa, I-56127 Pisa, Italy, <sup>A</sup>presently at INFN Sezione di Bologna, I-40127 Bologna, Italy

<sup>h</sup>INFN Sezione di Pisa, I-56127 Pisa, Italy

<sup>i</sup>IPHC, UMR 7178, Université de Strasbourg, CNRS, 67037 Strasbourg, France

<sup>j</sup>Indian Institute of Technology Madras, Chennai 600036, India

<sup>k</sup>Faculty of Mathematics and Physics, Charles University, 121 16 Prague, Czech Republic

<sup>l</sup>Malaviya National Institute of Technology Jaipur, Jaipur 302017, India

<sup>m</sup>Dipartimento di Fisica, Università di Trieste, I-34127 Trieste, Italy

<sup>n</sup>INFN Sezione di Trieste, I-34127 Trieste, Italy

<sup>o</sup>High Energy Accelerator Research Organization (KEK), Tsukuba 305-0801, Japan

<sup>p</sup>The Graduate University for Advanced Studies (SOKENDAI), Hayama 240-0193, Japan

<sup>q</sup>Kavli Institute for the Physics and Mathematics of the Universe, University of Tokyo, Kashiwa 277-8583, Japan

<sup>r</sup>Punjab Agricultural University, Ludhiana 141004, India

<sup>s</sup>Department of Physics, Kyungpook National University, Daegu 41566, Korea

\*Speaker

36 <sup>1</sup>*Aix Marseille Université , CNRS/IN2P3, CPPM, 13288 Marseille, France, <sup>B</sup>presently at INFN Sezione di*  
37 *Roma Tre, I-00185 Roma, Italy*

38 <sup>4</sup>*School of Physics, University of Melbourne, Melbourne, Victoria 3010, Australia*

39 *E-mail: [abdulbasith.kaliyar@oeaw.ac.at](mailto:abdulbasith.kaliyar@oeaw.ac.at)*

The Belle II silicon vertex detector (SVD) is a four-layer double-sided silicon strip detector installed within the Belle II detector located at KEK, Japan. The SVD has been operating smoothly and reliably since the start of data taking in March 2019. The data quality and radiation damage effects have been constantly monitored. In this article, we report the operational experience of SVD, reconstruction performance and effects of beam background and radiation damage. We also report some of the recent efforts to improve the software robustness targeting the high luminosity scenario and hardware activities performed during the first long shutdown of Belle II experiment.

## 1. Introduction

The Belle II experiment [1] aims to make precise measurements of weak-interaction parameters, study exotic hadrons, and search for physics beyond the Standard Model of particle physics. The experiment is currently underway at the SuperKEKB accelerator research center located in Tsukuba, Japan. SuperKEKB [2] is an asymmetric beam energy  $e^+$  (4 GeV)  $e^-$  (7 GeV) collider that operates at centre-of-mass energies near the  $\Upsilon(4S)$  resonance (10.58 GeV). The instantaneous peak luminosity achieved so far is  $4.7 \times 10^{34} \text{ cm}^{-2}\text{s}^{-1}$ , which is the current world record. The ultimate target is to reach a peak luminosity of  $6 \times 10^{35} \text{ cm}^{-2}\text{s}^{-1}$ . The Belle II detector, positioned around the collider interaction point, has so far collected  $430 \text{ fb}^{-1}$  of data. The eventual goal is to collect  $50 \text{ ab}^{-1}$  of data in the next decade.

The vertex detector (VXD) is the innermost subdetector in the Belle II detector system located closest to the interaction point. Comprising six layers, it includes two inner layers of pixel detector (PXD) [3], based on depleted field effect transistor sensors, and four outer layers of silicon strip detector, known as the silicon vertex detector (SVD) [4]. The SVD is crucial for extrapolating the measured tracks to the PXD and point at a region-of-interest that helps to significantly reduce the amount of data recorded by the PXD. Besides, the SVD also performs standalone tracking of low-momentum particles, vertex detection of  $K_S^0$  and  $\Lambda$  particles, and contributes to the charged-particle identification by providing energy-loss information.

In July 2022, Belle II temporarily paused operation for the first long shutdown to allow the accelerator maintenance and improvements to the detector. The VXD was re-installed during this time with a new complete PXD and the same SVD. In this article we present a detailed description of the SVD, its performance until July 2022, effects of radiation damage, the software improvements aimed towards high-luminosity running, and finally a report on the the VXD re-installation and commissioning during the long shutdown.

## 2. Belle II Silicon Vertex Detector

The Belle II SVD is composed of four layers of double-sided silicon strip detector (DSSD), namely layers 3, 4, 5 and 6, placed at radii of 39, 80, 104, and 135 mm, respectively, from the beam pipe. The material budget is about 0.7% of a radiation length per layer. In total, there are 172 sensors representing an area of  $1.2 \text{ m}^2$  and 224,000 readout strips. There are three types of DSSDs: small rectangular sensors in layer 3, large rectangular sensors in the barrel region of layers 4, 5, and 6, and slanted trapezoidal sensors to extend spacial coverage toward the forward region of these three outermost layers. These sensors are made from an N-type bulk 6-inch wafer with a thickness of about  $300 \mu\text{m}$ . To provide two-dimensional spatial information, P-side strips of the sensors are placed parallel to the beam axis, while N-side strips are placed transverse to it. The details of the DSSDs are summarized in Table 1. The readout strips are AC coupled and there is one intermediate floating strip between two readout implants. The full depletion voltage ranges from 20 – 60 V, and the operating voltage is 100 V. The radiation hardness of SVD sensors is about 6 Mrad.

The front-end readout ASIC used in SVD is APV25 [5], with 128 input channels. It collects signal from the strips and provides analog readout. APV25 has a fast 50 ns shaping time and a radiation hardness up to 100 Mrad. By default, the chip operates in multi-peak mode at a

**Table 1:** Details of the three types of DSSDs used in the SVD.

	Small rectangular	Large rectangular	Trapezoidal
Sensor active area (mm <sup>2</sup> )	122.90 × 38.55	122.90 × 57.52	122.76 × (38.42 – 57.59)
Number of P-strips	768	768	768
P-strip readout pitch (μm)	50	75	50 – 75
Number of N-strips	768	512	512
N-strip readout pitch (μm)	160	240	240
Thickness (μm)	320	320	300
Manufacturer	Hamamatsu	Hamamatsu	Micron

81 clock frequency of 31.8 MHz, which is 1/8th of the SuperKEKB bunch-crossing frequency. Six  
 82 consecutive samples are read out upon the arrival of a global hardware trigger to reconstruct the  
 83 signal pulses. To save data transmission bandwidth during high-luminosity runs, a 3/6-mixed  
 84 operation mode is developed, where three or six samples are acquired depending on the timing  
 85 precision of the hardware trigger. The 3/6-mixed operation mode has been tested and is ready to be  
 86 used in the future.

### 87 3. Operation and performance

88 The SVD has been operating smoothly and reliably since its installation in 2019. The total  
 89 fraction of masked strips due to defects is less than 1% and only one out of 1748 APV25s was  
 90 temporarily disabled. Temperature and calibration constants are evolving within the expected ranges  
 91 due to radiation damage. The hit efficiency exceeds 99% for all the sensors. Figure 1 shows example  
 92 of distributions of cluster charge and cluster signal-to-noise ratio (SNR) measured in 2022 and 2020.  
 93 The signal cluster charge is normalized to the track path length in the silicon to correct for the track’s  
 94 incidence angle. The normalized cluster charge is found to be in good agreement with expectations  
 95 and similar in all sensors. The charge matches the expected minimum ionizing particle value of  
 96 24000  $e^-$  within 15%, which is the uncertainty in the absolute APV25 gain calibration. The cluster  
 97 SNR is defined as the total cluster charge divided by the quadratic sum of the noise values from  
 98 each strip in the cluster. A small decrease of cluster SNR is observed in 2022 data, due to ~ 20% –  
 99 30% increased noise from radiation damage. In general, very good SNR is measured across all 172  
 100 DSSD sensors, with most probable values typically falling within the range of 13 to 30, depending  
 101 on sensor side and position.

102 The cluster-position resolution is crucial for vertexing and track reconstruction performance.  
 103 The position resolution of the SVD is estimated from the residual between the cluster position and the  
 104 unbiased track extrapolation, after subtracting quadratically the track extrapolation uncertainty [6].  
 105 Studies using dimuon ( $e^+e^- \rightarrow \mu^+\mu^-$ ) events show a resolution of 7 – 12 μm for the P-side and  
 106 15 – 25 μm for the N-side. These are in fair agreement with expectations from the sensor pitch.  
 107 Good stability of position resolution over the time is also confirmed by comparing measurements  
 108 from 2022 with that of 2020.

109 The SVD also offers an excellent hit time resolution. It is measured from the residuals of the  
 110 hit time with respect to the time of the  $e^+e^-$  collision provided by the central drift chamber of the

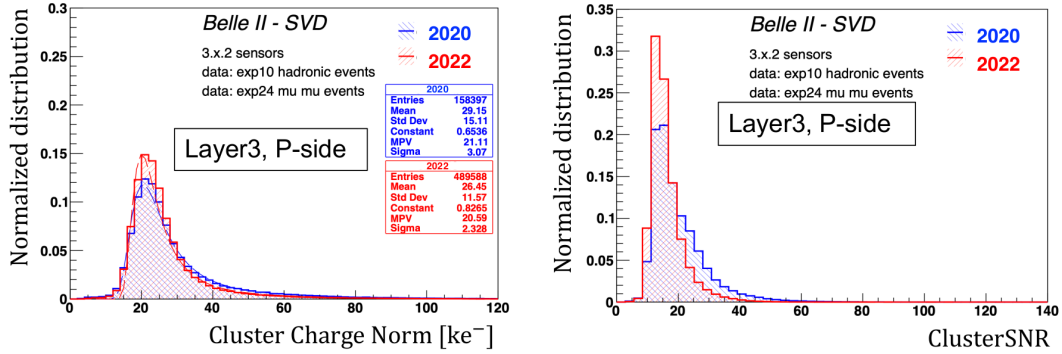


Figure 1: Distributions of signal cluster charge (left) and cluster SNR (right) for P-strips of a layer 3 sensor.

111 Belle II detector. The measured hit time resolution is 2.9 ns (2.4 ns) for the P (N) side. The hit-time  
 112 information is also used to remove the machine-related background, which is typically unassociated  
 113 with the  $e^+e^-$  collisions. This off-time-hit background enters the triggered data acquisition window  
 114 and increases the strip occupancy. Background occupancy above a certain threshold can cause  
 115 tracking performance degradation. Time difference between the P- and N- side clusters can also  
 116 be used to suppress the wrong combination of P- and N- side clusters in case of multiple particles  
 117 crossing the sensor. By requiring the cluster time within 50 ns of the event time and time difference  
 118 between P and N side cluster within 20 ns, 50% of the off-time background hits can be rejected  
 119 while keeping 99% tracking efficiency. This allows to set the hit occupancy limit of layer 3 to 4.7%  
 120 without tracking performance deterioration.

121 Two new algorithms are currently being developed that exploit the SVD time information  
 122 to further relax the hit-occupancy limit and enhance the offline software robustness in the high-  
 123 background environment. One method involves the selection of track-time, which is computed by  
 124 combining the hit-time of SVD clusters associated with a track. This reduces the fake-track rate,  
 125 thus relaxing the hit-occupancy limit. The second algorithm involves grouping SVD clusters using  
 126 the hit-time information. The cluster-time distribution has a clear grouping structure since clusters  
 127 from different bunches are collected within the acquisition time window of the triggered event.  
 128 Signal clusters are located in a group around the event time, while other background hits form other  
 129 groups, which are caused by other beam-bunches. However, the hit-time selection cannot help to  
 130 eliminate background hits present within the 50 ns range. The cluster grouping method allows  
 131 event-by-event classification and further background elimination. The addition of these two new  
 132 algorithms allow to set the hit-occupancy limit at around 6%. Further software improvement and  
 133 optimization are currently ongoing before incorporating these features in the actual data processing.

#### 134 4. Beam background and radiation effects

135 In this section we discuss the effects of radiation damage on the SVD sensors during its  
 136 operation. The beam-induced background increases the hit occupancy and causes radiation damage  
 137 to the sensors. The radiation damage affects the strip noise, leakage current, and full depletion

138 voltage of sensors and it is constantly monitored during the operation. Current average hit occupancy  
139 on layer-3 sensors is less than 0.5% and well under control. The radiation dose in the SVD is  
140 estimated based on the data from diamond sensors that are mounted on the beam pipe and the  
141 bellows pipes outside of the VXD. The total integrated radiation dose on layer-3 sensors is 70 krad,  
142 which corresponds to an equivalent 1 – MeV neutron fluence of  $1.6 \times 10^{11}$  n<sub>eq</sub>/cm<sup>2</sup>, assuming the  
143 ratio of a neutron fluence to a radiation dose of  $2.3 \times 10^9$  n<sub>eq</sub>/cm<sup>2</sup>/krad based on MC simulation.

144 The strip noise, which is dominated by the inter-strip capacitance, increased by about 20%  
145 (30%) during the operation for N-side (P-side), which is expected to be saturated. The leakage  
146 current is gradually increasing and, in general, its value shows a linear dependence on the accumu-  
147 lated dose, as expected from non-ionising energy loss model [7]. So far, this increase has negligible  
148 contribution to the noise because of small leakage current and short APV25 shaping time. However,  
149 after 6 Mrad the leakage current contribution to the noise might become significant and thus, this  
150 reduce the SNR below 10 in the layer-3. So far no changes in full depletion voltage are observed in  
151 the operating sensors.

152 Further studies have been carried out with several irradiation campaigns to better evaluate the  
153 radiation tolerance of SVD sensors even after bulk-type inversion. In July 2022, a new irradiation  
154 campaign of SVD sensors was performed with 90 MeV  $e^-$  beam at the Research Center for  
155 ELectron Photon Science in Tohoku University, with a radiation dose up to 10 Mrad (corresponding  
156 to a neutron fluence of  $3 \times 10^{13}$  n<sub>eq</sub>/cm<sup>2</sup>). The type inversion of the sensor bulk is confirmed after  
157 2 Mrad of radiation. The tests confirm that the SVD sensor works well even after the bulk type  
158 inversion, as expected from previous experience of silicon detectors of similar type. These results  
159 provide a large safety margin for SVD even after a decade-long operation at target luminosity.

## 160 **5. VXD reinstallation during Long Shutdown 1**

161 In July 2022, Belle II paused its operation for the first long shutdown to allow the accelerator  
162 maintenance and implement upgrades to the detector. A brand new pixel detector (PXD2) with  
163 a complete second layer was installed in the VXD volume along with the current SVD. Very  
164 intense hardware activities were carried out involving the SVD crew during the de-installation and  
165 re-installation of the VXD. On 10 May, 2023, the VXD was safely extracted from the Belle II  
166 detector, followed by dismounting two SVD half-shells from the old PXD and mounting them on  
167 the PXD2. All these delicate operations involved several steps with extensive testing of the detector  
168 and the environmental monitoring system, to ensure the healthiness of the system after each step.  
169 The healthiness of all SVD sensors was confirmed during the commissioning of the new VXD in  
170 the clean room. In July, 2023, the new VXD was successfully reinstalled into the Belle II detector.  
171 Additional tests including cosmic ray runs were performed before the start of the actual beam  
172 operation. After this shutdown, Belle II officially restarted data taking in January 2024, and so far  
173 SVD is performing as smoothly as before.

## 174 **6. Conclusion**

175 The Belle SVD has been taking high-quality data since March 2019. Operation is stable and  
176 reliable with excellent detector performance. Effects from radiation damage are observed at the

177 expected level, however their contribution does not cause any degradation to the SVD tracking  
178 performance so far. During the first long shutdown, a new VXD was successfully re-installed into  
179 the Belle II detector incorporating the full PXD2 together with the existing SVD.

180 Background extrapolation to the targeted high luminosity as well as the results of irradiation  
181 campaign show that the SVD is expected to remain safe even after a decade of operation. However,  
182 the high-background environment in the future may deteriorate tracking performance of the SVD  
183 as indicated by the simulation studies. Not only to enhance the robustness against high background,  
184 but also to adapt to a possible modification of the interaction region, technology assessment is  
185 ongoing for a possible VXD upgrade during the second long shutdown of the Belle II operation  
186 [8–10].

## 187 7. Acknowledgements

188 This project has received funding from the European Union’s Horizon 2020 research and  
189 innovation programme under the Marie Skłodowska-Curie grant agreements No 644294, 822070  
190 and 101026516 and ERC grant agreement No 819127. This work is supported by MEXT, WPI  
191 and JSPS (Japan); ARC (Australia); BMBWF (Austria); MSM (Czechia); CNRS/IN2P3 (France);  
192 AIDA-2020 (Germany); DAE and DST (India); INFN (Italy); NRF and RSRI (Korea); and MNiSW  
193 (Poland).

## 194 References

- 195 [1] T. Abe, *et al.*, (Belle-II Collaboration), Belle II Technical Design Report [[arXiv:1011.0352](https://arxiv.org/abs/1011.0352)].
- 196 [2] Y. Ohnishi, *et al.*, Prog. Theor. Exp. Phys. **2013**, 03A011 (2013).
- 197 [3] B. Wang, *et al.*, (Belle-II DEPFET and PXD Collaborations), Nucl. Instrum. Meth. A **1032**,  
198 166631 (2022).
- 199 [4] K. Adamczyk, *et al.*, (Belle-II SVD Collaboration) JINST **17**, P11042 (2022).
- 200 [5] M. J. French, *et al.*, Nucl. Instrum. Meth. A **466**, 359 (2001).
- 201 [6] R. Leboucher, *et al.*, Nucl. Instrum. Meth. A **1033**, 166746 (2022).
- 202 [7] G. Lindström, M. Ahmed, *et al.*, Nucl. Instrum. Meth. A **465** (2001) 60–69, sPD2000.
- 203 [8] Belle-II Collaboration, Snowmass Whitepaper: The Belle II Detector Upgrade Program,  
204 [[arXiv:2203.11349](https://arxiv.org/abs/2203.11349)] (2022).
- 205 [9] M. Babeluk, *et al.*, Nucl. Instrum. Meth. A **1048** 168015 (2023).
- 206 [10] A. Ishikawa, *et al.*, Nucl. Instrum. Meth. A **978**, 164404 (2020).